Calibration of DSF model for real-time control

Calibration of DSF model for real-time control

Calibration of DSF model for real-time control

G. Gennaro[1,2], F. Favoino[1], F. Goia[3], G. De Michele[2] and M. Perino[1]

[1]TEBE research group, Energy Dept., Politecnico di Torino, Turin, Italy
[2]EURAC Research, Bozen, Italy
[3]Norwegian University of Science and Technology, NTNU, Trondheim, Norway

Abstract. Double Skin Façades are complex fenestration systems capable to control solar heat gain and ventilation in buildings. Due to the high flexibility of such innovative components, having energy models able to replicate the thermal behaviour of the Double Skin Facades is of utmost importance for their optimal control and integration with building automation strategies. In this context, a numerical model has been developed and validate within the experimental data. The methodological steps are presented in this work and in the last section, the potential applications of the model are discussed.

1. Introduction

Double Skin Façades are advanced building envelopes that could give a balanced behavior across different building domains such as energy use, thermal comfort, visual comfort and indoor air quality.

This technology has reached high degrees of maturity which have led to the development of increasingly flexible Double Skin Facades (DSF), which are able to optimize everchanging building requirements (i.e. indoor thermal and visual comfort, energy demand, etc.) with intrinsically dynamic boundary conditions (climate, occupancy) [1]. The flexibility of the DSF is made possible by the control of the different actuators (i.e. ventilation openings, cavity fans, solar shadings etc.) enabling the achievement of multiple façade configurations. Therefore, a decision-making system is of utmost importance to ensure that the DSF is controlled in a proper way to achieve the required building performance target. In literature, it has been highlighted that to effectively control such façade technology it is essential to accurately predict the contribution that this element has in the overall building thermal balance (in terms of solar gains, thermal and ventilation loads) [2].

From a modelling point of view, different approaches can be used to replicate the thermal behavior of DSFs: regarding the white box-model, they vary in order of complexity from simplified model to dynamic models. The simplified models are based on lumped-parameter in steady-state condition and the DSF performance is described with conventional metrics (e.g. U-value, g-value). The dynamic models, instead, are advanced model which can be stand-alone or integrated in BES tools (e.g. Airflow Window for EnergyPlus and Type 56_CFS for TRNSYS). However, these tools exhibit poor accuracy of the results on component level variables (e.g. surface temperature, air gap temperature) and they are not suitable for implementing model-based controls due to computational costs [3]. On the other hand, data-driven models are playing an important role also for the implementation of building controls when it comes to complex and dynamic façade elements. This approach does not explicit the relation between the different variables through physic-based relationships but on statistically-based correlations trained on an extended dataset. Therefore, the dataset needs to be large and rich (covering all the possible operational envelopes) to guarantee the robustness and accuracy of this kind of models [4].

In these contexts, the present paper aims to exhibit a numerical model representing the thermal behavior of the DSF control-oriented. Therefore, the model has been meant to be streamlined, flexible and easly parametrizable. The simplified model is based on a lumped-parameter thermal network according to the Standard ISO 15099-2003 [5] and it allows to evaluate the thermal performance at the DSF component, solving a set of first-order equations. Indeed the numerical model has very short computational times, allowing the model to be integrated in an embedded single board controller within the DSF itself, and the models outputs to be seamlessly integrated in a building level supervisory system. The simplified model has been validated and tested with the measured data acquired during the experimental campaign carried out on a DSF prototype installed in the South-exposed façade of the outdoor test facility at Energy Department of Politecnico di Torino [6].

2. Case study and methodology

The DSF prototype (Fig. 1) has been developed with the aim to maximize the flexibility of the façade, which adapts to the boundary conditions, can minimize the building energy uses while guaranteeing high levels of indoor comfort. The prototype consists of two parallel transparent skins within an aluminium framing system, presenting an equally sized (1.22 m wide for 2.00 m high) Double Glazing Unit (DGU, 6 mm thick with low emissivity coating on the internal surface of the DGU cavity, and 16 mm gap filled with a mixture of air and 90% Argon). The parallel skins form a 25 cm thick air cavity, containing four vertical fans (nominal flow 220 m^3/h each) placed at 2.6 m height, to increase the ventilation flow when required. To control the air path between the indoor and outdoor environment, four ventilation openings (1.5 m x 0.5 m) are placed on the inner (bottom and top) and outer (bottom and top) skin, which can be opened independently to achieve different air path within the DSF cavity as described in [1]. Within the DSF, an embedded single board controller (Raspberry Pi 4) is devoted to the task of actuation (fan velocity, opening percentage of the different vents in an independent way, height and angle of the Venetian blind) and sensing main environmental parameters (i.e. outdoor and indoor air temperature, incident and transmitted solar radiation, cavity air temperature, indoor air temperature and vertical and horizontal internal illuminance). In addition to the single-board controller, a measurement system is deployed within the test facility to reliably and accurately monitor the main outdoor, indoor and façade physical parameters, by means of Modbus protocol for data acquisition and storage. In detail (Fig. 1) the following measured variables are acquired with a 30 seconds frequency and averaged every 5 minutes: local weather data (i.e. outdoor air temperature, horizontal and vertical global irradiance, wind velocity and wind direction), DSF data (i.e. heat-fluxes and window surface

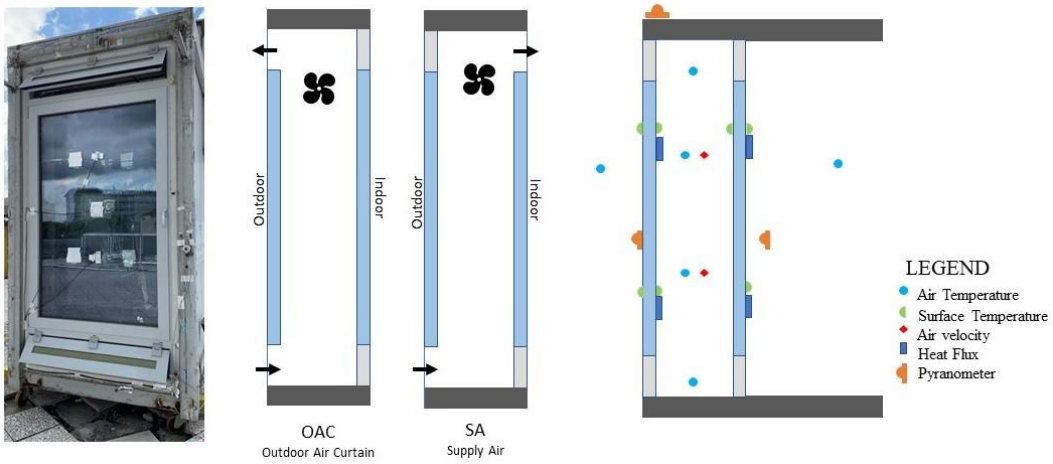

Figure 1. *DSF prototype in OAC configuration (left),OAC and SA configuration (center), sensor scheme (right)*

temperature of the different layer at two different levels, cavity inlet and outlet air temperature, cavity air velocity and temperature, transmitted vertical global irradiance) and test facility data (indoor air temperature and surface temperatures).

The dataset used in this work refers to the DSF in the configurations of Outdoor Air Curtain (OAC) and Supply Air (SA). For both the configuration, outdoor air enters the DSF's cavity from the bottom inlet; for the OAC configuration the cavity air is released to the outdoor (this configuration is usually adopted to minimize the solar gains through the DSF); for the SA configuration, the cavity air is released to the indoor space to provide (preheated) outdoor air for ventilation purpose (Fig. 1). For both configurations, both natural and mechanical ventilation modes have been characterized.

3. DSF modelling through the ISO 15099 Standard

The ISO 15099 Standard is a detailed calculation standard used to calculate the thermal and optical performance of windows. The standard is the basis of free tools (i.e. WIS software and WINDOW) useful for the calculation of the thermal and solar properties of Double Skin Facades (U-value, g-value, surface temperatures). However, such software do not allow the user to modify the source code, thus limiting the calibration of the models and its possible implementations. Conversely, the writing of the model structure in Python language makes it more flexible, enabling for example the introduction of additional model parameters to improve the accuracy of the model (during the calibration steps), or the implementation on a single board controller to build a model-based decision making.

In this section, only the main equations related to the energy balance and the DSF airflow characterization are presented, while the reader is redirected to the ISO 15099-2003 for the detailed algorithms and mathematical models, the same nomenclature has been used to facilitate understanding. The following assumptions have been set up for the development of the simplified model (the first three are in line with the ISO 15099 hypothesis): (i) the only centre of glazing properties are adopted, (ii) the heat transfer is assumed to be one-dimensional, (iii) no capacitive nodes are considered, and (iv) the inner and outer skins of the façade are considered as single layers having the equivalent thermal and optical characteristics of the overall DGU (pre-calculated through WINDOW 7.7).

The calculation of the thermal properties is based on a heat transfer model, with analysis of coupled conductive, convective and radiative heat transfer. The conductive heat transfer within each layer can be described using first-principles calculation. Convection heat transfer is modelled using heat transfer correlation, while the radiation exchange is computed using the view factor based radiosity method and implemented in a layer-by-layer approach. Figure 2 shows the glazing system, consisting of 3 layers subjecting to the set of boundary conditions. Each layer is described with three longwave optical properties: the front and back emissivities, $\varepsilon_{f,i}$ and $\varepsilon_{b,i}$ and the transmittance τ_i.

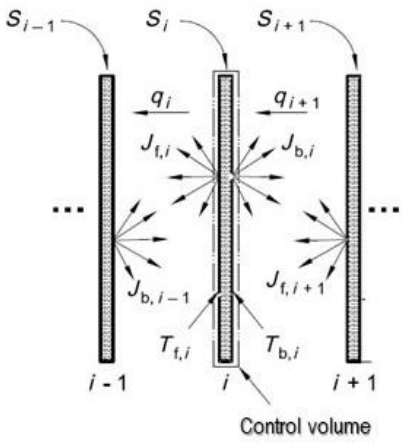

Figure 2 *Energy balance on the control volume[5]*

The energy balance on the control volume of the glazing layer *i* allows the calculation of the density of heat flow rate q_i *:*

$$q_i = h_{c,i}\left(T_{f,i} - T_{b,i-1}\right) + J_{f,i} - J_{b,i-1} \tag{1}$$

where, $h_{c,i}$ is the convective exchange coefficient between surface and surface [W/m^{2}K], $J_{f,i}$ and $J_{b,i-1}$ the radiosity of layer *i* on the front side and of layer *i-1* on the back side [W/m^2] respectively and $T_{f,i}$ and $T_{b,i-1}$ the temperature of glazing *i* on the front side and of glazing i-1 on the back side [K], respectively.

The following four equations need to be solved for each layer *i* to calculate the temperature at each glazing surface and corresponding radiosities:

$$q_i = S_i + q_{i+1} \tag{2.1}$$

$$J_{f,i} = \varepsilon_{f,i}\sigma T_{f,i}^4 + \tau_i J_{f,i+1} + \rho_{f,i} J_{b,i-1} \tag{2.2}$$

$$J_{b,i} = \varepsilon_{b,i}\sigma T_{b,i}^4 + \tau_i J_{b,i-1} + \rho_{b,i} J_{f,i-1} \tag{2.3}$$

$$T_{b,i} - T_{f,i} = \frac{t_{g,i}}{2\,k_{g,i}}(2\,q_{i+1} + S_i) \tag{2.4}$$

where, S_i is the heat flow rate of absorbed solar radiation at the *i-th* layer [W/m^2], $t_{g,i}$ is the i-th layer thickness [m] and $k_{g,i}$ its conductivity [W/mK].

When the cavity of the façade is ventilated, it is necessary to introduce the term due to ventilation $q_{v,i}$ added directly to the cavity gap node. The convective heat transfer coefficient for heat transfer inside faces of glasses in the cavity to cavity air is calculated as follows:

$$h_{cv,i} = 2h_{c,i} + 4v_i \tag{3}$$

The air velocity in the cavity is caused by the stack effect and depends on the driving pressure difference and the resistance to the airflow of the opening and space itself. The driving pressure difference is approximated as follow:

$$\Delta p_{i,k} = \rho_0 * T_0 * g * H_i * \frac{|T_{gap,i} - T_{gap,k}|}{T_{gap,i} * T_{gap,k}} \tag{4}$$

where $T_{gap,i}$ is the mean temperature of the air in the cavity, $T_{gap,k}$ is the mean temperature of the connected space and T_0 is the reference temperature [K]. The airflow in the cavity is modelled as a pipe flow and therefore the driving force is set equal to the total pressure loss (sum of Bernoulli pressure loss, Hagen-Poiseuille pressure loss and pressure loss in the inlet and outlet openings). It is therefore clear that the model has an inter-dependence between the gap air temperature and the air velocity. Consequently, for the calculation of these two unknown variables, an iterative calculation is performed until the convergence limit of 1% is achieved.

4. Model calibration: parameters,procedure and performance assessment

The model described above has been implemented to describe the thermal behavior of the DSF prototype in OAC and SA configuration. As shown from the comparison of the blue line (representing the uncalibrated model) and the dashed black line (representing the measured data) in Fig 3, a calibration process was necessary in order to improve the fitness of the data predicted by the numerical model with the measured data. In particular, the calibration is based on the comparison of four DSF parameters which determine the total heat flux exchanged through the façade: the outlet air temperature (T_{outlet}) and air cavity velocity (v) for characterizing the ventilative heat exchange through the air cavity of the DSF; the innermost lass surface temperature, T inner glass (T_{inlet}) and the DSF cavity air gap temperature (T_{gap}) for characterizing the convective and radiative heat exchange through the DSF.

Two statistical indicators have been used to compare quantitatively the fitness of the model with the experimental data: Mean Bias Error (MBE) and the Root Mean Square Error (RMSE) defined as follow:

$$MBE = \frac{\sum_{i=1}^{n}\left(X_{sim} - X_{exp}\right)_i}{n} \tag{5.1}$$

$$RMSE = \sqrt{\frac{\sum_{i=1}^{n}(X_{sim}-X_{exp})i^2}{n}} \quad (5.2)$$

where X_{sim} is the predicted value by the simulation, X_{exp} the measured value and n the total number of measurements. The one-step-ahead technique has been used, proceeding for 7 intermediate steps described in Table 1, in which the indices (5.1) and (5.2) have been minimized.

Fig. 4 shows the improvement that each calibration step has made to the model: more improvements are due to the step 2 and 5 in which the convective coefficient of the DGU and the DSF cavity have been tripled respect to the starting value, respectively. By comparing the measured data with those simulated by the model, an anomalous distribution of the surface temperatures of the single skin was found: the temperature layers facing the cavity was too high while those facing outward has a lower temperature. This could be related to the assumption made for the development of the model in which the double-glazing unit have been model as a single layer with fixed cavity resistance values independent from the boundary conditions [6]. Therefore, to overcome this simplification, the convective exchange coefficient inside the DGU gap has been increased as follow (Table 1, step 2):

$$h_{s,i} = k_2 \cdot h_{gl,i} + h_{r,i} \quad (6.1)$$

$$R_{g,i} = 2\frac{t_{g,i}}{k_{g,i}} + \frac{1}{h_{s,i}} \quad (6.2)$$

In step 5 instead, the air gap temperature simulated was higher than measured, so the contribution of convection inside the cavity has been increased as follow (Table 1, step 5):

$$h_{c,i} = Nu_i \frac{k_{g,i}}{t_{g,i}} k_5 \quad (7)$$

where Nu_i is the dimensionless Nusselt number. In addition, the outdoor air temperature has been used as radiative boundary condition instead of the mean radiative temperature (Table 1, step 4) as follow:

$$E_{ex} = \sigma T_{ex}^4 \quad (8)$$

where, E_{ex} is the external irradiance [W/m^2] and T_{ex} the outdoor air temperature [K]. Moreover, the data analysis has evidenced a time lag between the peak of the measured data with the peak of simulated ones and therefore, at each timestep, the one-hour early incident solar radiation is considered since the ISO model is only resistive and not capacitive (Table 1, step 1). As a final step, the cavity inlet air temperature has been modified considering the sol-air temperature instead of the outdoor air temperature (in both configurations the air is taken from the outside) as follows:

$$T^*_{gap,in} = T_{gap,in} + k_6 \frac{I_s}{h_{c,e} + h_{r,e}} \quad (9)$$

This assumption results from the fact that the ventilation openings are made of a mixed aluminum and wood material which during the day heats up and pre-heat the inlet air. For only mechanical ventilation cases, it was noted that the trend of air velocity inside the cavity was not constant during the sunny hours, but they exhibit a trend similar to the natural case (Fig. 3). For this reason, the air speed has been corrected by considering the root of the sum of the square of the fan speed v_{fan} and the velocity due to the stack effect v_{nat}, multiplied with the calibration factor k_7:

$$v^*_{fan} = \sqrt{\left({v_{nat}}^2 * k_7 + {v_{fan}}^2\right)} \quad (10)$$

This final step involves a considerable improvement, grouping the points of the scatter plots within the confidence area equal to the ±1°C and ±0.05 m/s for temperatures and air velocity, respectively (Fig. 4). It should be noted that the calibration coefficients (k_2, k_5, k_6, k_7) are the results of a sub-calibration process in which each parameter k_i is varied within a specific calibration range, as shown in Table 1 (the parameter which is finally adopted, leading to an improvement in terms of the statistical parameters from equations (5.1) and (5.2), is shown in bold).

Table 1. Steps for the calibration model. For column 'calibration range' the value chosen is shown in bold.

# Step	Description	Initial parameter	Final parameter	Calibration range
0	Uncalibrated ISO model	-	-	-
1	One-hour early incident solar radiation	$Q_{inc}(t)$	$Q_{inc}(t-1)$	-
2	Increase in the internal convective heat transfer coefficient of the DGU	$h_{gl,i}$	$k_2\ h_{gl,i}$	[1,2, **3**, 4,5]
3	Heat losses due to frame and infiltration	T_{gap}	$T_{gap} + f(\dot{Q}_{inf} + \dot{Q}_{frame})$	-
4	Outdoor temperature as the convective boundary condition	T_{mr}	T_{ex}	-
5	Increase of the internal convective heat transfer coefficient DSF cavity	$h_{c,i}$	$k_5\ h_{c,i}$	[1,2, **3**, 4,5]
6	Sol-air temperature as inlet air temperature	$T_{gap,in}$	$T_{gap,in} + \frac{k_6\ Q_s}{h_{c,e} + h_{r,e}}$	[0.1, **0. 2**, 0.3]
7	Sum of velocity in quadrature for mechanical ventilation	v_{fan}	$v^*_{fan} = \sqrt{({v_{nat}}^2 * k_7 + {v_{fan}}^2)}$	[0.1, **0. 2**, 0.3,0.4]

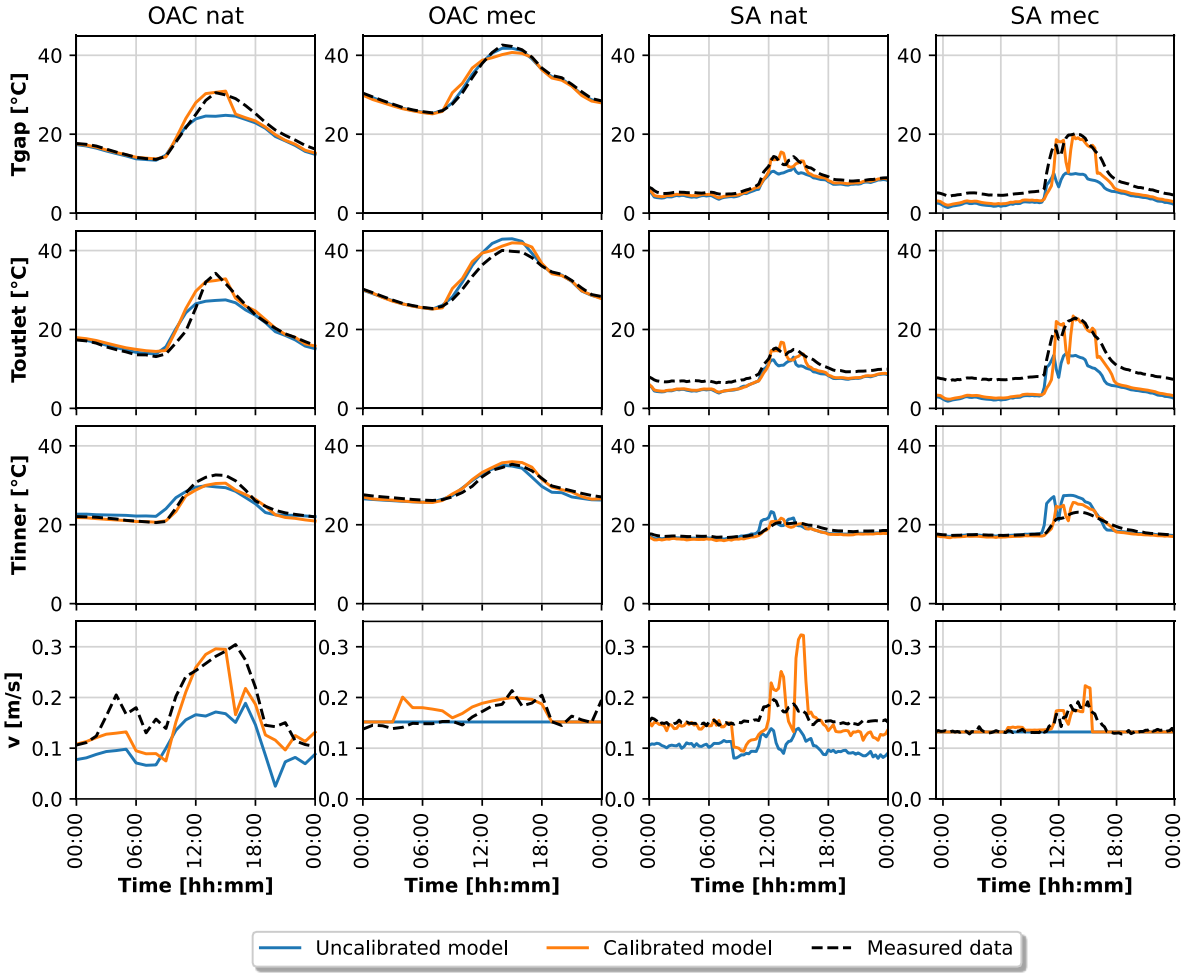

Figure 3 *Comparison between pre-calibrated and calibrated model though measured data for DSF in OAC and SA configuration both natural (nat) and mechanical (mec) ventilated*

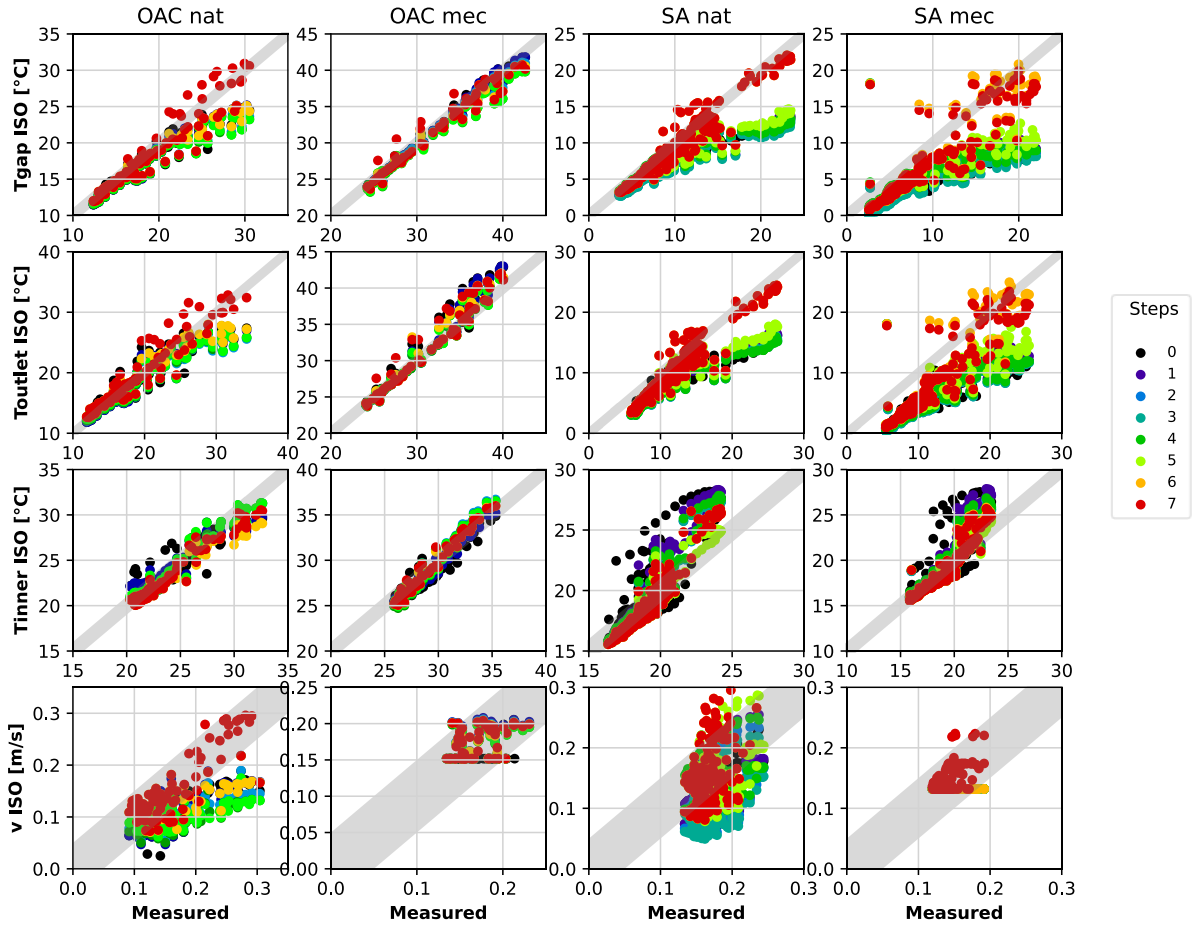

Figure 4 *Scatter plot measured vs simulated of (from top to bottom) air gap temperature, outlet temperature, internal window surface temperature and air velocity with confidence area in grey for (from left to right) OAC and SA configuration, natural and mechanical ventilated. Improvement at each calibration step.*

5. Discussion and conclusion

Fig. 3 qualitatively compares the pre-and post- calibrated model data series within the measured ones for both Outdoor Air Curtain and Supply Air ventilation modes, for both natural and mechanical ventilation. In all cases, this calibration procedure has led to the development of a simplified model of the DSF, which considers the same k_i calibration parameters.

The calibrated model is more accurate in predicting the air cavity temperature - outlet and gap - (due to dedicated calibration steps, and particularly the ones which allowed to modify the cavity air gap and the inlet temperature, respectively step 2 and 5), but it exhibits lower accuracy for the internal surface temperature. This could be due to the simplifying hypothesis of modelling the DGU as a single layer with equivalent overall thermal and integral optical properties, which also led to the underestimation of the convective heat transfer coefficient within the insulated glazing unit cavity. This can be improved by increasing the number of nodes representing the DGU within the model.

Moreover, Fig. 3 shows that some of the configurations are less accurate during the night hours - more evident during the SA dataset acquired during winter 2021 (OAC dataset refers to summer 2020). This could be due to the only resistive nature of the model, which does not have any capacitive node thus ignores the thermal inertia of the glazing systems. The calibration approach presented could be generalizable even in the absence of experimental data: the parameters introduced during the calibration

derive from physical assumptions (Steps 1, 3, 6, 7); in the remaining steps, instead, the parameters were considered to compensate for some simplifications introduced in the model.

The simplified numerical model of the DSF above presented is based on the resolution of a set of first-order equations and iterative cycles. These features make the computational costs very low and therefore allows the implementation of this simplified model on single board controllers which could be embedded in the façade, so that it could be used to perform parametric simulation and optimisation to inform control decision making of the DSF system, and coordinated with the building supervisory system, so to achieve the overall building performance targets (e.g. energy savings and indoor thermal comfort). Different real-time control strategies can be implemented using this simplified model: for example, the model should be used to run parametric simulation varying the DSF configurations. Therefore, starting from the parametric results the controller will choose the DSF configuration that allows the achievement of the performance targets. This is a brute force approach in which the controller makes a parametric simulation of all DSF configurations at each timestep. To reduce the number of the DSF configurations (and thus improve the computational performance of such approach), a decision-tree could be used to filter the number of the DSF possible configuration of the parametric analysis. In alternative, the simplified model could be used in an optimization control logic: due to the low computational times, the model is well suited for the use with optimizers which through predictive features can calculate the best sequence of future DSF configurations to minimize a given cost function during an optimization horizon (e.g. MPC).

Nevertheless, it is a component level model, describing only the heat flow through the façade, which has its advantages, such as the possibility to be used independently for the estimation of the thermal loads and surface temperature within a decentralised controller, and its disadvantages, such as the fact that it does not evaluate the performance of the environment behind the façade, and should therefore be coupled with a zone (or building) thermal model. Moreover, the model could also be used in a co-simulation framework, to estimate the air velocity in the ventilated cavity, which can then be adopted within a DSF model of BES software.

The potential of the presented model, therefore, could represent a starting point towards the design and implementation of more complex advanced model-based controls, which could further improve the operational performance of highly flexible Double Skin Façades.

6. Acknowledgements

The authors thank the student Fabio Cassinelli for his contribution to this work within his MSc thesis.

7. Reference

1. Catto Lucchino E, Goia F, Lobaccaro G and Chaudhary G. Modelling of double skin facades in whole-building energy simulation tools: A review of current practices and possibilities for future developments. Build Simul. 2019;3–27.
2. Gennaro G, Goia F., De Michele G., Perino M. and Favoino F., Embedded single-board controller by dynamic transparent facades: a co-simulation virtual testbed. Accepted in the Proceeding of BS2021 Conference, 1-3 September 2021. Bruges, Belgium.
3. Catto Lucchino E, Gelesz A, Skeie K, Gennaro G, Reith A, Serra V, et al. Modelling double skin façades (DSFs) in whole-building energy simulation tools: Validation and inter-software comparison of a mechanically ventilated single-story DSF. Build Environ. 2021;199.
4. Kathirgamanathan A, De Rosa M, Mangina E and Finn DP. Data-driven predictive control for unlocking building energy flexibility: A review. Renew Sustain Energy Rev . 2021;135:110120.
5. Standardisation IO for. Thermal performance of windows, doors and shading devices - detailed calculations (ISO 15099). 2003;
6. Goia F and Serra V. Analysis of a non-calorimetric method for assessment of in-situ thermal transmittance and solar factor of glazed systems. Sol Energy. 2018;166:458–71.